PHYSICAL REVIEW A **109**, L040801 (2024)

Letter

Many-body theory calculations of positron binding to halogenated hydrocarbons

J. P. Cassidy,[1,*] J. Hofierka,[1] B. Cunningham,[1] C. M. Rawlins,[1] C. H. Patterson,[2] and D. G. Green[1,†]
[1]*School of Mathematics and Physics, Queen's University Belfast, University Road, Belfast BT7 1NN, United Kingdom*
[2]*School of Physics, Trinity College Dublin, Dublin 2, D02 PN40, Ireland*

(Received 31 August 2023; accepted 7 March 2024; published 22 April 2024)

Positron binding energies in halogenated hydrocarbons are calculated *ab initio* using many-body theory. For chlorinated molecules, including planars for which the interaction is highly anisotropic, very good to excellent agreement with experiment and recent density-functional-theory-based model-potential calculations is found. Predictions for fluorinated and brominated molecules are presented. The comparative effect of fluorination, chlorination, and bromination is elucidated by identifying trends within molecular families including dihaloethylenes and halomethanes based on global molecular properties (dipole moment, polarizability, ionization energy). It is shown that relative to brominated and chlorinated molecules, fluorinated molecules generate a less attractive positron-molecule potential due to larger ionization energies and smaller density of molecular orbitals close to the highest occupied molecular orbital, resulting in very weak, or in most cases loss of, positron binding. Overall, however, it is shown that the global molecular properties are not universal predictors of binding energies, exemplified by consideration of CH_3Cl vs *cis*-$C_2H_2F_2$: Despite the latter having a larger dipole moment, lower ionization energy, and similar polarizability, its binding energy is significantly smaller (25 vs 3 meV, respectively), owing to the important contribution of multiple molecular orbitals to, and the anisotropy of, the positron-molecule correlation potential.

DOI: 10.1103/PhysRevA.109.L040801

Trap-based positron beams have enabled resonant-annihilation-based measurements of positron binding energies for around 90 molecules [1–10]. While the corresponding theory of positron capture into vibrational Feshbach resonances is well established [2,11,12], accurate calculations of positron binding energies have been realized only relatively recently (see, e.g., Refs. [7,13–23]). Attempts have been made to relate the observed binding energies to the global molecular properties including the dipole moment μ, isotropic polarizability α, and ionization potential I [3,5,20], but no such accurate universal formula has yet been found. Recently, we developed an *ab initio* many-body theory (MBT) approach that quantified the role of strong many-body correlations, and beyond the interplay of the global properties, highlighted the importance of individual molecular orbital contributions to the positron-molecule potential, e.g., the enhancement of binding due to π bonds [19,21] that was also deduced from experiment [3,9,10]. We have also extended it to positron binding in ringed hydrocarbons [22], positron scattering and annihilation in atoms and small molecules [24,25], and to predict new positronically bonded molecules [26].

Also recently, a model-polarization-potential method [16] was used to calculate binding in chlorinated hydrocarbons, in a joint theory-experimental study [7]. Although good agreement was found with experiment for many of the molecules considered, for planar molecules the calculations substantially overestimated the measured binding energies, with the suggestion that this was due to the model assuming an isotropic long-range positron-molecule interaction [27]. By contrast, density-functional-theory (DFT)-model calculations for planar chloroethylenes [19] accounted for the anisotropy approximately and found better overall agreement with experiment. The method relied on an adjustable gradient parameter β, whose value the authors of Ref. [19] were able to choose to replicate the binding energies of dichloroethylenes to within around 10 meV, but this value led to underestimated binding energies for tri- and tetrachloroethylene, at worst by 30 meV. The anisotropy of the positron-molecule potential, not captured by the global molecular properties, is thus important, and *ab initio* calculations are demanded for a fundamental understanding and description of the body of experimental data.

The purpose of this Letter is twofold. First, we apply our many-body theory approach [28] to study positron binding in the chlorinated hydrocarbons considered in the recent model calculations [7,19] and experiment [7], accounting for the positron-molecule correlations and anisotropic potential *ab initio*. We find very good (excellent in cases) agreement with experiment and DFT-based model calculations, including for the planar molecules. Second, we go beyond the previous chlorinated studies [7,19] and make predictions for fluorinated and brominated molecules, and elucidate the com-

---

[*] jcassidy18@qub.ac.uk
[†] d.green@qub.ac.uk

parative effects of fluorination, chlorination, and bromination. We find that compared to their brominated and chlorinated counterparts, fluorinated molecules generate a successively less attractive positron-molecule potential resulting in very weak or loss of binding. We identify trends in binding based on global molecular properties (α, μ, and I) for families including the sequences of *cis*/(Z)-dihaloethylenes $C_2H_2Br_2 \rightarrow C_2H_2BrCl \rightarrow C_2H_2Cl_2 \rightarrow C_2H_2ClF \rightarrow C_2H_2F_2$ [29], and halomethanes. However, we find the global properties to be poor universal indicators of binding energies, exemplified by CH_3Cl and *cis*-$C_2H_2F_2$ which have similar α, μ, and I but significantly different positron binding energies (25 vs 3 meV). We explain this and the overall results, and provide further fundamental insight by considering the individual molecular orbital (MO) contributions to the positron-molecule correlation potential, showing that e.g., the decrease (or loss of) binding for bromination → chlorination → fluorination is due to successively higher molecular orbital ionization energies and smaller density of states close to the highest occupied molecular orbital (HOMO).

Theoretical approach. A detailed description of our MBT approach is given in Ref. [21]. Briefly, we solve the Dyson equation [30,31] $(\hat{H}_0 + \hat{\Sigma}_\varepsilon)\psi_\varepsilon(\mathbf{r}) = \varepsilon\psi_\varepsilon(\mathbf{r})$ self-consistently for the positron wave function $\psi_\varepsilon(\mathbf{r})$ with energy ε. Here, $\hat{H}_0$ is the zeroth-order Hamiltonian of the positron in the static (Hartree-Fock) field of the molecule and $\hat{\Sigma}_\varepsilon$ is the positron self energy (an energy-dependent, nonlocal correlation potential) [32]. We calculate it using a diagrammatic expansion in electron-electron and electron-positron interactions (see Fig. 1 of Ref. [21]), involving three main diagram classes: the *GW* diagram, which describes polarization, screening of the electron-positron Coulomb interaction, and electron-hole interactions; the virtual-positronium (vPs) formation ladder series, which describes the temporary tunneling of an electron to the positron, denoted Σ^{Γ}; and the positron-hole repulsion ladder series, denoted Σ^{Λ}. The significant enhancement and enabling of binding due to these correlations were delineated in Ref. [21]. Here, we quote results only for our most sophisticated self-energy $\Sigma^{GW+\Gamma+\Lambda}$ [33].

We expand the electron and positron wave functions in Gaussian basis sets, using augmented correlation-consistent polarized valence X zeta (aug-cc-pVXZ) bases [X = triple (T), quadruple (Q)] [34] on atomic centers as well as additional hydrogen aug-cc-pVXZ bases on "ghost" centers 1 Å from the molecule to resolve regions of maximum positron density. For all of the molecules considered, we placed five ghosts around each halogen atom in the molecule in the shape of a square-pyramidal cap, with each ghost 1 Å from the halogen. We also use diffuse even-tempered positron bases of the form $10s9p8d7f6g$, with exponents $\zeta_0 \times \beta^{k-1}$ ($\zeta_0 = 0.000\,01$–0.006 and $\beta = 2$–3), ensuring the positron is described well at large distances $r \sim 1/\kappa$, where $\kappa = \sqrt{2\varepsilon_b}$ [for further details on basis sets used, see Supplemental Material (SM) [35]]. For molecules with >2 chlorines the positron wave function is delocalized (Fig. 1), and we found that an accurate description of the vPs contribution requires a prohibitively large basis set [36] (for our current computing resources), and our *ab initio* calculations are not converged, though are lower bounds. Thus we also performed MBT-based model calculations approximating $\Sigma \approx g\Sigma^{(2)} + \Sigma^{(\Lambda)}$, using the second-order self-energy scaled to approximate the virtual-Ps contribution as introduced and justified in Ref. [21]: *Ab initio* calculations give g in the range 1.4–1.5 for the HOMOs [see Ref. [21] and also Fig. 2(d)]. This approach still calculates the anisotropic polarization potential *ab initio*, but is much less computationally expensive.

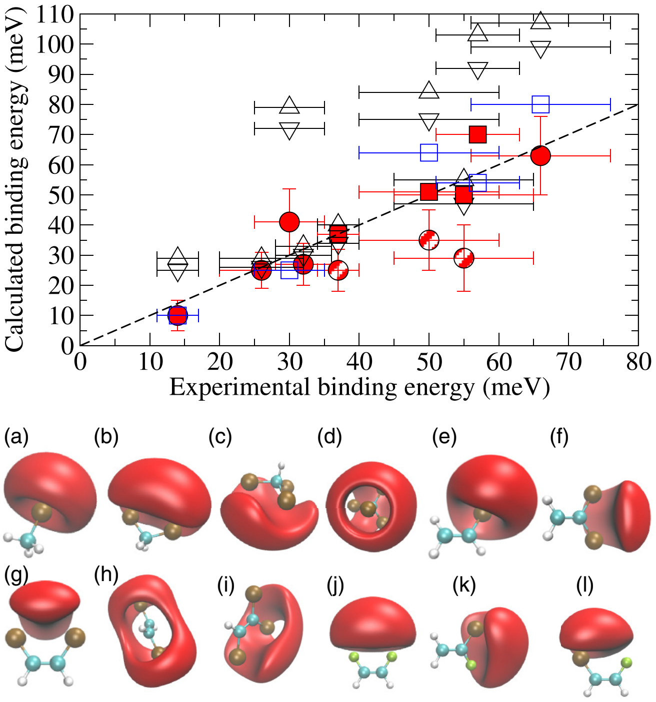

FIG. 1. Top: Calculated positron binding energies compared with experiment for chlorinated molecules. Present MBT (red circles, and striped circles for molecules difficult to converge *ab initio*); MBT-based model calculations using $\Sigma = g\Sigma^{(2)} + \Sigma^{\Lambda}$ with $g = 1.5$ (red squares); (isotropic) polarization potential model calculation of Ref. [7] (black triangles; two for each molecule reflecting two choices of cutoff parameter); DFT-model calculation of Ref. [19] (blue squares). Vertical error bars are plus-minus the maximum difference of our calculations using screened Coulomb interactions and *GW*@RPA (random phase approximation) MO energies vs bare Coulomb interactions and HF MO energies [21]. Bottom: Positron (Dyson) wave function at 80% maximum for chlorinated and fluorinated molecules with $\varepsilon_b \geqslant 1$ meV. (a) Chloromethane; (b) dichloromethane; (c) trichloromethane; (d) tetrachloromethane (at 93%); (e) vinyl chloride; (f) vinylidene chloride; (g) *cis*-1,2-dichloroethylene; (h) *trans*-1,2-dichloroethylene (at 90%); (i) trichloroethylene; (j) *cis*-1,2-difluoroethylene; (k) 1-chloro-1-fluoroethylene; (l) (Z)-chlorofluoroethylene.

Chlorinated molecules: Comparison with experiment and model calculations. Our calculated positron binding energies ε_b for the chlorinated hydrocarbons considered in the recent isotropic-polarization-potential (IPP) [7] and DFT-model calculations [19] and experiment [7], and our predictions for their fluorinated and (select) brominated counterparts are presented in Table I. Figure 1 summarizes this for the chlorinated molecules, and also presents the calculated bound-state positron Dyson orbitals for chlorinated and select chlorofluorinated molecules, showing that the positron localizes around the halogens. Overall, very good agreement is found between

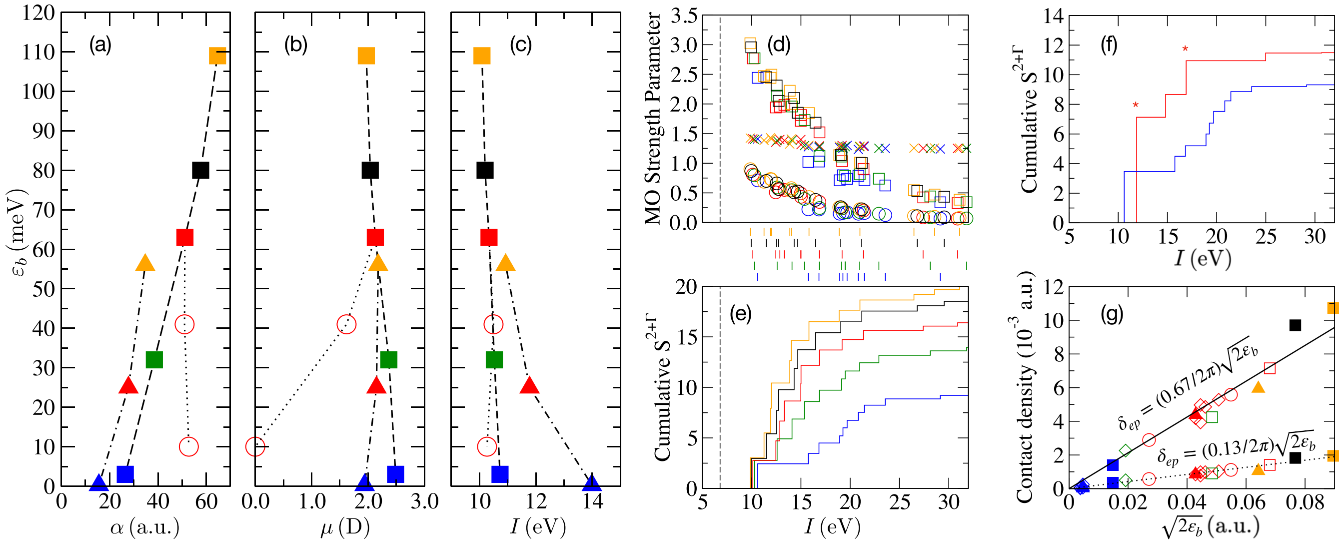

FIG. 2. Dependence of positron binding energies on global molecular properties and individual MOs. (a)–(c) Calculated ε_b vs calculated polarizabilities, dipole moments, and ionization energy for the brominated (orange), bromochlorinated (black), chlorinated (red), chlorofluorinated (green), and fluorinated (blue) molecules; symbols denote molecular families; squares are *cis*-dihaloethylenes C_2H_2XY, triangles are halomethanes CH_3X (X, Y = Br, Cl, F), and circles are isomers of $C_2H_2Cl_2$. Dashed lines are guides; (d) the positron-molecule correlation strength parameters $\mathcal{S}_n^{\Gamma}$ (circles) and $\mathcal{S}_n^{2+\Gamma}$ (squares), and the ratio $g_n \equiv \mathcal{S}_n^{2+\Gamma}/\mathcal{S}_n^{2}$ (crosses) for each MO n against the MO HF ionization energies (vertical lines between panels) for the *cis*-dihaloethylenes sequence [colors as in (a)–(c)]. (e) The corresponding cumulative $\mathcal{S}^{2+\Gamma}$ obtained by summing from the HOMO to the core orbitals. (f) The cumulative strength $\mathcal{S}^{2+\Gamma}$ for CH_3Cl (red; asterisks denote double degeneracy) and *cis*-$C_2H_2F_2$ (blue). (g) The calculated unenhanced ($\gamma_i = 1$) and enhanced contact densities for molecules with a $\Sigma^{GW+\Gamma+\Lambda}$ bound state. Colors and symbols as in (a)–(c), and diamonds are remaining molecules from Table I.

the *ab initio* MBT calculations and experiment. For CH_3Cl, our calculated $\varepsilon_b = 25$ meV is in excellent agreement with both experiment and the IPP model calculations [an absolute (relative) error of only 1 meV (4%)]. We find excellent agreement with experiment (i.e., $\leqslant 5$ meV absolute error) for CH_2Cl_2, and for *cis*-$C_2H_2Cl_2$ (for which both the IPP and DFT models substantially overestimate) and *trans*-$C_2H_2Cl_2$, and reasonable agreement (11 meV above experiment) for vinylidene chloride $C_2H_2Cl_2$. Overall, our *ab initio* results are in good agreement with the DFT-based calculations [19] (including vinyl chloride, for which there is no measurement). The results of the MBT-based model calculation, which importantly augment our unconverged *ab initio* results for the molecules with >2 chlorines, are presented in the final column of Table I. The model calculations with $g \sim 1.5$ generally give excellent agreement with experiment (with the exception of ethylene).

Fluorinated molecules: Predictions. Compared to the chlorinated molecules, in the fluorinated counterparts we find (see Table I) that positron binding is either lost or greatly reduced (as explained in the next section). We predict bound states for fluoromethane, difluoroethylene, vinyl fluoride (a few tenths of a meV each), and *cis*-1,2-difluoroethylene ($\varepsilon_b \sim 3$ meV). Although fluoromethane is known to be vibrational Feshbach resonance (VFR) active, ε_b was found to be too small to measure [37]. However, our prediction of a weak bound state for fluoromethane of ~0.3 meV is in agreement with that derived from the Z_{eff} fit of the annihilation spectrum of CH_3F, which until now had not been corroborated with any theoretical calculations [38]. This contradicts a recent machine-learning-based prediction that fluoromethane does not bind a positron [20]. Our prediction of a bound state for CH_2F_2 with $\varepsilon_b = 0.2$ meV concurs with the 0.4 meV prediction by an earlier empirical model [3]. Our lack of binding in CF_4 is consistent with experiment; this molecule is known to not be VFR active [37]. We also considered 1-chloro-1-fluoroethylene and (*Z*)-chlorofluoroethylene, and report binding energies of 5 and 32 meV. These values lie between the fully chlorinated and fluorinated binding energies (see below).

Comparative effect of fluorination, chlorination, and bromination; the role of MO energies and density of states. Figures 2(a)–2(c) show the calculated ε_b as a function of the global molecular properties α, μ, and I for the dihaloethylenes (*cis*/*Z*-C_2H_2XY and the isomers of $C_2H_2Cl_2$) and halomethanes CH_3X, where X, Y = F, Cl, or Br. These present three distinct cases. Across the *cis*-dihaloethylenes I and μ vary weakly, and the increase in ε_b going from $X, Y = F_2 \rightarrow ClF \rightarrow \cdots \rightarrow Br_2$ follows an increase in α: In a given family a more polarizable target is more attractive to the positron. Across the halomethanes, μ is almost constant, and the increase in ε_b going from F to Br follows both an increasing α and decreasing I (the less tightly bound electrons are more susceptible to perturbation from the positron). For the isomers of $C_2H_2Cl_2$, α and I vary weakly, and the decrease in ε_b from *cis*-$C_2H_2Cl_2$ to vinylidene chloride to the nonpolar *trans*-$C_2H_2Cl_2$ is due to successively decreasing μ. These three distinct cases highlight that the global molecular properties can explain trends in ε_b for families of molecules, but they are not reliable universal predictors of binding energies, as exemplified by considering CH_3Cl and *cis*-$C_2H_2F_2$. These have very similar α, but while *cis*-$C_2H_2F_2$ has a larger μ and

TABLE I. Calculated MBT positron binding energies (meV) for halogenated hydrocarbons compared with experiment and model-potential calculations. For calculations denoted "<0" binding was not observed. Where $\varepsilon_b < 1$ meV, we quote values to one decimal place. Molecules marked "*" are those for which we believe our *ab initio* calculations to be unconverged and we recommend the model-MBT result (final column, see text). Also shown are calculated HF dipole moments, isotropic dipole polarizabilities [calculated at the *GW*@BSE (Bethe-Salpeter equation) level] and ionization energies (calculated at the *GW*@RPA level and used in the energy denominators of the self-energy analytic expressions [21]). Numbers in bold correspond to our recommended calculated value for each molecule.

					Present *ab initio* MBT		Model-potential calculations		
Molecule	Formula	μ (D)	α (a.u.)	I (eV)	$\Sigma^{GW+\Gamma+\Lambda}$	Expt. [7]	IPP[a]	DFT[b]	Present MBT-based model[c]
Methane	CH_4	0	13.83	14.18	<0		<0		<0
Chloromethane	CH_3Cl	2.15	27.80	11.78	**25**	26 ± 6	29, 26		8–23
Dichloromethane	CH_2Cl_2	1.83	40.61	11.93	**27**	32 ± 4	34, 30		15–31
Trichloromethane*	$CHCl_3$	1.19	53.34	11.95	25*	37 ± 3	40, 34		16–**37**
Tetrachloromethane*	CCl_4	0	64.14	12.02	29*	55 ± 10	55, 47		22–**50**
Ethylene	C_2H_4	0	24.40	10.75	1	20 ± 10	5		<0
Vinyl chloride	C_2H_3Cl	1.68	38.67	10.57	**27**		54, 50	27	8–28
Vinylidene chloride	$C_2H_2Cl_2$	1.62	51.04	10.50	**41**	30 ± 5	79, 72	25	13–30
cis-1,2-dichloroethylene	$C_2H_2Cl_2$	2.13	51.18	10.34	**63**	66 ± 10	107, 99	80	43–75
trans-1,2-dichloroethylene	$C_2H_2Cl_2$	0	52.79	10.27	**10**	14 ± 3	29, 25	10	2–12
Trichloroethylene*	C_2HCl_3	1.01	64.84	10.16	35*	50 ± 10	84, 75	64	23–**51**
Tetrachloroethylene	C_2Cl_4	0	87.02	9.46		57 ± 6	103, 92	54	34–70
1-chloro-1-fluoroethylene	C_2H_2ClF	1.49	38.46	10.71	**5**				2–10
(*Z*)-chlorofluoroethylene	C_2H_2ClF	2.37	38.52	10.53	**32**				22–39
Fluoromethane	CH_3F	1.94	15.56	13.99	**0.3**	0.3[d]			0.2–0.6
Difluoromethane	CH_2F_2	2.09	16.15	13.70	**0.2**				0.1–0.3
Trifluoromethane	CHF_3	1.75	16.66	15.17	<0				
Tetrafluoromethane	CF_4	0	17.13	16.26	<0	[e]			
Vinyl fluoride	C_2H_3F	1.47	26.11	10.92	**0.3**				0–0.6
Vinylidene fluoride	$C_2H_2F_2$	1.30	26.22	10.88	<0				
cis-1,2-difluoroethylene	$C_2H_2F_2$	2.49	26.50	10.73	**3**				1–7
trans-1,2-difluoroethylene	$C_2H_2F_2$	0	26.25	10.68	<0				
Trifluoroethylene	C_2HF_3	1.37	26.43	10.75	<0				
Bromomethane	CH_3Br	2.18	34.75	10.93	**56**	40[f]			23–41
cis-1,2-dibromoethylene	$C_2H_2Br_2$	1.97	64.67	10.09	**109**				58–108
(*Z*)-bromochloroethylene	C_2H_2BrCl	2.04	57.72	10.20	**80**				42–87

[a] Model-polarization-potential calculations of Swann and Gribakin, assuming an isotropic asymptotic interaction [7].

[b] DFT is the density-functional theory using the Perdew-Burke-Ernzerhof exchange functional result from Suzuki *et al.* [19].

[c] Using a scaled self-energy $\Sigma = g\Sigma^{(2)} + \Sigma^{(\Lambda)}$ with g ranging from 1.4 to 1.5 to account for vPs formation [21].

[d] Molecule is VFR active, but ε_b is too small to measure [37]. 0.3 meV was derived from the $Z_{\rm eff}$ fit of the VFR-based annihilation spectrum [38].

[e] CF_4 is not VFR active [37].

[f] From Ref. [37], where the uncertainty in the $Z_{\rm eff}$ peak positions from which ε_b was measured was reported to be between 10 and 15 meV.

lower I, it has a lower binding energy (3 vs 25 meV). To explain this, and the reduction or lack of binding in fluorinated molecules in general, we consider the individual molecular orbital contributions to the correlation potential. We do so via the strength parameter $\mathcal{S} = -\sum_\nu \langle\nu|\hat{\Sigma}_\varepsilon|\nu\rangle/\varepsilon_\nu$ [21,39], where ν is an excited positron Hartree-Fock (HF) orbital of energy ε_ν, with the self-energy taken as $\Sigma \approx \Sigma^{(2+\Gamma)}$, i.e., the sum of the bare polarization $\Sigma^{(2)}$ and the virtual-Ps $\Sigma^{(\Gamma)}$ diagrams. Figure 2(d) shows $\mathcal{S}^{(\Gamma)}$, $\mathcal{S}^{(2+\Gamma)}$, and the ratio $g = \mathcal{S}^{(2+\Gamma)}/\mathcal{S}^{(2)}$ for individual MOs as a function of the MO energy for the sequence of *cis*-dihaloethylenes: The strength parameters mainly decrease with increasing MO ionization energy because more tightly bound orbitals are more difficult for the positron to perturb [21]. Additionally, Fig. 2(e) shows the cumulative $\mathcal{S}^{(2+\Gamma)}$ obtained by summing from the HOMO to the core orbitals. Moving from $C_2H_2Br_2$ through to $C_2H_2F_2$ sees both the total $\mathcal{S}^{(2+\Gamma)}$ and the density of states near the ionization energy decrease; e.g., in $C_2H_2F_2$ there is a ~5 eV gap between the HOMO and the HOMO − 1, while this gap is approximately half as wide for $C_2H_2Cl_2$ and C_2H_2ClF and half as wide again for $C_2H_2Br_2$. Further, the contributions to the cumulative $\mathcal{S}^{(2+\Gamma)}$ below the HOMO for $C_2H_2F_2$ are smaller than those for the other three molecules as the MOs have larger I. In general, the transition from Br to Cl to F either shifts all the energy states to more negative energies, or at least drives the sub-HOMO energies further from the HOMO energy, inhibiting the molecule's ability to bind the positron (SM Fig. S1 [35] shows MO energies of all molecules considered). We now consider CH_3Cl and *cis*-$C_2H_2F_2$ [red triangle and blue square in Figs. 2(a)–2(c)]. Figure 2(f) shows their cumulative $\mathcal{S}^{(2+\Gamma)}$ strength parameter. We see that although CH_3Cl has a larger I, its HOMO is doubly degenerate, and contributes relatively more to the strength than the singly degenerate HOMO of CH_2F_2 (a second doubly degenerate state of π character also contributes strongly at ∼17 eV for CH_3Cl). Thus, in spite of CH_3Cl having a smaller dipole moment (which governs the strength of the static potential [40]), its larger correlation potential (which contributes to binding nonlinearly; see extended data Fig. 3 of Ref. [21]) ultimately results in stronger binding.

Annihilation and contact densities. The positron bound-state annihilation rate $\Gamma(\text{ns}^{-1}) = 50.47\delta_{ep}(\text{a.u.})$, where $\delta_{ep} = \sum_{i=1}^{N_e/2} \gamma_i \int |\varphi_i(\mathbf{r})|^2 |\psi_\varepsilon(\mathbf{r})|^2 d^3\mathbf{r}$ is the electron-positron contact density. Here, φ_i is the ith electron MO, ψ is the positron bound-state wave function (see, e.g., Fig. 1) renormalized to $a = (1 - \partial\varepsilon/\partial E|_{\varepsilon_b})^{-1} < 1$ [21], and $\gamma_i \geqslant 1$ are vertex enhancement factors that account for short-range electron-positron attractions [41,42]. We found that they followed $\delta_{ep} = (F/2\pi)\sqrt{2\varepsilon_b}$ [12] with $F = 0.67$, remarkably close to $F \approx 0.66$ for atoms [12] [see Fig. 2(g)].

Summary. Many-body theory calculations of positron binding to chlorinated hydrocarbons were found to be in good to excellent agreement with experiment and recent model-potential-based DFT calculations. Additionally, new predictions elucidated the comparative effects of fluorination, chlorination, and bromination: Trends within molecular families based on the global molecular properties μ, α, and I were identified, as was the importance of describing the positron-molecule potential anisotropy. Further, the importance of accounting for the energies and density of electron states (at least near the HOMO) when trying to explain trends in binding between different molecular families was highlighted, and we suggest that any accurate universal formula for positron binding energies should thus account for these properties. As well as providing fundamental insight, our results provide benchmarks and can inform other computational approaches to the positron-molecule and many-electron problems.

Relevant data files can be found at the Queen's University Data Repository [43]. The EXCITON+ code is available from the authors on reasonable request.

Acknowledgments. We thank James Danielson, Cliff Surko, Sarah Gregg and Andrew Swann for useful discussions, and additionally Gleb Gribakin for comments on the draft manuscript. This work was funded by the European Research Council Grant No. 804383 "ANTI-ATOM" (D.G.G.) and a DfE Northern Ireland postgraduate research studentship (J.P.C.), and used the NI HPC Service and the ARCHER2 U.K. National Supercomputing Service.

---

[1] S. J. Gilbert, L. D. Barnes, J. P. Sullivan, and C. M. Surko, Vibrational-resonance enhancement of positron annihilation in molecules, Phys. Rev. Lett. **88**, 043201 (2002).

[2] G. F. Gribakin, J. A. Young, and C. M. Surko, Positron-molecule interactions: Resonant attachment, annihilation, and bound states, Rev. Mod. Phys. **82**, 2557 (2010).

[3] J. R. Danielson, J. A. Young, and C. M. Surko, Dependence of positron-molecule binding energies on molecular properties, J. Phys. B: At. Mol. Opt. Phys. **42**, 235203 (2009).

[4] J. R. Danielson, J. J. Gosselin, and C. M. Surko, Dipole enhancement of positron binding to molecules, Phys. Rev. Lett. **104**, 233201 (2010).

[5] J. R. Danielson, A. C. L. Jones, J. J. Gosselin, M. R. Natisin, and C. M. Surko, Interplay between permanent dipole moments and polarizability in positron-molecule binding, Phys. Rev. A **85**, 022709 (2012).

[6] J. R. Danielson, A. C. L. Jones, M. R. Natisin, and C. M. Surko, Comparisons of positron and electron binding to molecules, Phys. Rev. Lett. **109**, 113201 (2012).

[7] A. R. Swann, G. F. Gribakin, J. R. Danielson, S. Ghosh, M. R. Natisin, and C. M. Surko, Effect of chlorination on positron binding to hydrocarbons: Experiment and theory, Phys. Rev. A **104**, 012813 (2021).

[8] J. R. Danielson, S. Ghosh, and C. M. Surko, Influence of geometry on positron binding to molecules, J. Phys. B: At. Mol. Opt. Phys. **54**, 225201 (2021).

[9] S. Ghosh, J. R. Danielson, and C. M. Surko, Resonant annihilation and positron bound states in benzene, Phys. Rev. Lett. **129**, 123401 (2022).

[10] J. R. Danielson, S. Ghosh, and C. M. Surko, Enhancement of positron binding energy in molecules containing π bonds, Phys. Rev. A **106**, 032811 (2022).

[11] G. F. Gribakin, Mechanisms of positron annihilation on molecules, Phys. Rev. A **61**, 022720 (2000).

[12] G. F. Gribakin, Theory of positron annihilation on molecules, in *New Directions in Antimatter Chemistry and Physics*, edited by C. M. Surko and F. A. Gianturco (Springer, Dordrecht, 2001), pp. 413–435.

[13] M. Tachikawa, Y. Kita, and R. J. Buenker, Bound states of the positron with nitrile species with a configuration interaction multi-component molecular orbital approach, Phys. Chem. Chem. Phys. **13**, 2701 (2011).

[14] M. Tachikawa, Positron-attachment to acetonitrile, acetaldehyde, and acetone molecules: Vibrational enhancement of positron affinities with configuration interaction level of multi-component molecular orbital approach, J. Phys.: Conf. Ser. **488**, 012053 (2014).

[15] J. Romero, J. A. Charry, R. Flores-Moreno, M. T. do N. Varella, and A. Reyes, Calculation of positron binding energies using the generalized any particle propagator theory, J. Chem. Phys. **141**, 114103 (2014).

[16] A. R. Swann and G. F. Gribakin, Calculations of positron binding and annihilation in polyatomic molecules, J. Chem. Phys. **149**, 244305 (2018).

[17] A. R. Swann and G. F. Gribakin, Positron binding and annihilation in alkane molecules, Phys. Rev. Lett. **123**, 113402 (2019).

[18] A. R. Swann and G. F. Gribakin, Model-potential calculations of positron binding, scattering, and annihilation for atoms and small molecules using a Gaussian basis, Phys. Rev. A **101**, 022702 (2020).

[19] H. Suzuki, T. Otomo, R. Iida, Y. Sugiura, T. Takayanagi, and M. Tachikawa, Positron binding in chloroethenes: Modeling positron-electron correlation-polarization potentials for molecular calculations, Phys. Rev. A **102**, 052830 (2020).

[20] P. H. R. Amaral and J. R. Mohallem, Machine-learning predictions of positron binding to molecules, Phys. Rev. A **102**, 052808 (2020).

[21] J. Hofierka, B. Cunningham, C. M. Rawlins, C. H. Patterson, and D. G. Green, Many-body theory of positron binding to polyatomic molecules, Nature (London) **606**, 688 (2022).

[22] E. Arthur-Baidoo, J. R. Danielson, C. M. Surko, J. P. Cassidy, S. K. Gregg, J. Hofierka, B. Cunningham, C. H. Patterson, and D. G. Green, Positron annihilation and binding in aromatic and other ring molecules, arXiv:2312.02779.

[23] J. Hofierka, B. Cunningham, and D. G. Green, Many-body theory calculations of positron binding to hydrogen cyanide, Eur. Phys. J. D **78**, 37 (2024).

[24] C. M. Rawlins, J. Hofierka, B. Cunningham, C. H. Patterson, and D. G. Green, Many-body theory calculations of positron scattering and annihilation in H_2, N_2, and CH_4, Phys. Rev. Lett. **130**, 263001 (2023).

[25] J. Hofierka, C. M. Rawlins, B. Cunningham, D. T. Waide, and D. G. Green, Many-body theory calculations of positron scattering and annihilation in noble-gas atoms via the solution of Bethe-Salpeter equations using the Gaussian-basis code EXCITON+, Front. Phys. **11**, 1227652 (2023).

[26] J. P. Cassidy, J. Hofierka, B. Cunningham, and D. G. Green, Many-body theory calculations of positronic-bonded molecular dianions, J. Chem. Phys. **160**, 084304 (2024).

[27] Specifically, their model constructed the positron-molecule potential as a sum of positron-atom potentials, using a hybrid polarizability of an atom in a certain chemical environment. At long range the IPP takes the isotropic asymptotic form $-\alpha/2r^4$; while this is true for spherical-top molecules, the true asymptotic form of the polarization potential is generally anisotropic, and is given by $-1/2r^6 \sum x_i x_j \alpha_{ij}$, where x_i are the Cartesian coordinates and α_{ij} are the Cartesian components of the polarizability tensor [16,19].

[28] We use the fixed-nuclei approximation: Compared to the correlations, vibrational effects have been found to have a relatively small effect on the binding energy [14,15,21,44–46].

[29] Here, the descriptor (Z) refers to $(E)/(Z)$ isomerism, where (Z) means that the highest priority groups, (i.e., the halogen atoms) are on the same side of the C-C double bond.

[30] W. H. Dickhoff and D. V. Neck, *Many-Body Theory Exposed! - Propagator Description of Quantum Mechanics in Many-Body Systems*, 2nd ed. (World Scientific, Singapore, 2008).

[31] A. L. Fetter and J. D. Walecka, *Quantum Theory of Many-Particle Systems* (Dover, New York, 2003).

[32] J. S. Bell and E. J. Squires, A formal optical model, Phys. Rev. Lett. **3**, 96 (1959).

[33] We use screened Coulomb interactions in the ladder diagrams and MO energies calculated in the random phase approximation. The ε_b in this approximation are found to be within 4 meV of those calculated using bare Coulomb interactions and HF MO energies for chlorinated and brominated molecules (maximum relative error of 7.4%), and 0.1 meV for fluorinated molecules.

[34] R. A. Kendall, T. H. Dunning Jr., and R. J. Harrison, Electron affinities of the first-row atoms revisited. Systematic basis sets and wave functions, J. Chem. Phys. **96**, 6796 (1992).

[35] See Supplemental Material at http://link.aps.org/supplemental/10.1103/PhysRevA.109.L040801 for further details on the basis sets and ghost placements used, values of the positron Dyson orbital renormalization constants, effect of halogenation on the molecular orbital energies and density of states, and calculated Z_{eff} spectrum for CH_3Br.

[36] The vPs contribution to the self-energy requires diagonalization of dense matrices of size $(N_+N_-)^2$, where N_+ (N_-) is the number of virtual positron (electron) states used. For example, our C_2HCl_3 calculations have $N_+N_- = 280\,800$, corresponding to 630 GB of memory. With other memory costs considered, our approach regularly requires more than 1 TB of memory.

[37] J. A. Young and C. M. Surko, Feshbach-resonance-mediated positron annihilation in small molecules, Phys. Rev. A **78**, 032702 (2008).

[38] G. F. Gribakin and C. M. R. Lee, Positron annihilation in molecules by capture into vibrational Feshbach resonances of infrared-active modes, Phys. Rev. Lett. **97**, 193201 (2006).

[39] V. A. Dzuba and G. F. Gribakin, Correlation-potential method for negative ions and electron scattering, Phys. Rev. A **49**, 2483 (1994).

[40] G. F. Gribakin and A. R. Swann, Effect of dipole polarizability on positron binding by strongly polar molecules, J. Phys. B **48**, 215101 (2015).

[41] D. G. Green and G. F. Gribakin, γ-ray spectra and enhancement factors for positron annihilation with core electrons, Phys. Rev. Lett. **114**, 093201 (2015).

[42] D. G. Green and G. F. Gribakin, Enhancement factors for positron annihilation on valence and core orbitals of noble-gas atoms, in *Concepts, Methods and Applications of Quantum Systems in Chemistry and Physics*, edited by Y. Wang, M. Thachuk, R. Krems, and J. Maruani, Progress in Theoretical Chemistry and Physics, Vol. 31 (Springer, Cham, 2018), pp. 243–263.

[43] Queen's University Data Repository, 10.17034/c682299e-3d9c-4b67-9c39-c70d210da575.

[44] F. A. Gianturco, J. Franz, R. J. Buenker, H.-P. Liebermann, L. Pichl, J.-M. Rost, M. Tachikawa, and M. Kimura, Positron binding to alkali-metal hydrides: The role of molecular vibrations, Phys. Rev. A **73**, 022705 (2006).

[45] R. J. Buenker and H. Libermann, Role of the electric dipole moment in positron binding to the ground and excited states of the BeO molecule, J. Chem. Phys. **126**, 104305 (2007).

[46] R. J. Buenker and H.-P. Liebermann, Configuration interaction calculations of positron binding to molecular oxides and hydrides and its effect on spectroscopic constants, Nucl. Instrum. Methods Phys. Res., Sect. B **266**, 483 (2008).